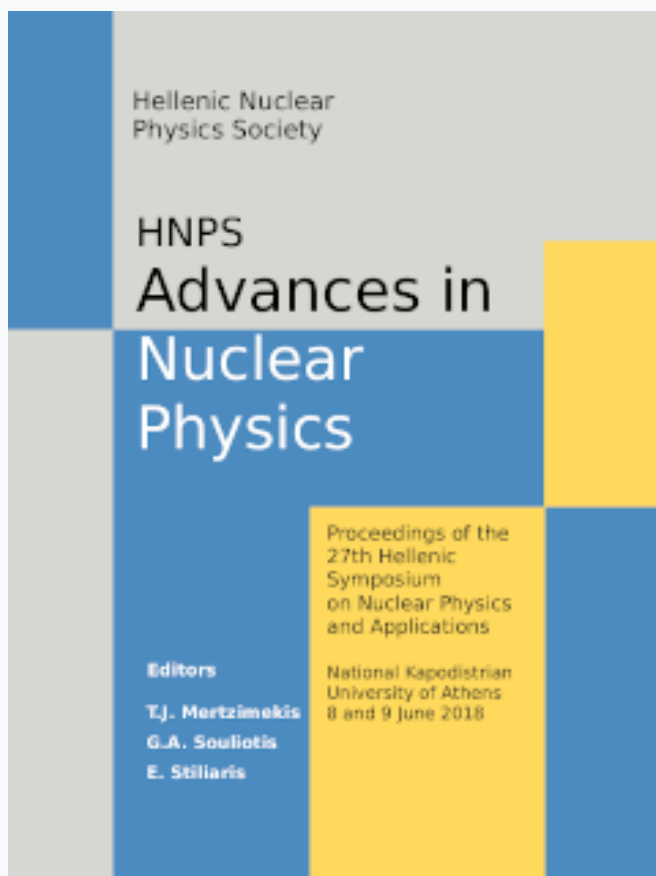


HNPS Advances in Nuclear Physics

Vol 26 (2018)

HNPS2018



Rare Isotope Production in peripheral heavy-ion collisions at beam energy of 15 MeV/nucleon

O. Fasoula, G. A. Souliotis, K. Tshoo, S. C. Jeong, B. H. Kang, Y. K. Kwon, M. Veselsky, A. Bonasera

doi: [10.12681/hnps.1821](https://doi.org/10.12681/hnps.1821)

To cite this article:

Fasoula, O., Souliotis, G. A., Tshoo, K., Jeong, S. C., Kang, B. H., Kwon, Y. K., Veselsky, M., & Bonasera, A. (2019). Rare Isotope Production in peripheral heavy-ion collisions at beam energy of 15 MeV/nucleon. *HNPS Advances in Nuclear Physics*, 26, 201–209. <https://doi.org/10.12681/hnps.1821>

Rare Isotope Production in peripheral heavy-ion collisions at beam energy of 15 MeV/nucleon

O. Fasoula^a, G.A. Souliotis^{a,*}, K. Tshoo^b, S.C. Jeong^b,
B.H. Kang^b, Y.K. Kwon^b, M. Veselsky^c, A. Bonasera^{d,e}

^a *Laboratory of Physical Chemistry, Department of Chemistry, National and Kapodistrian University of Athens, Athens, Greece*

^b *The Rare Isotope Science Project (RISP), Institute for Basic Science, Daejeon, Korea.*

^c *Institute of Physics, Slovak Academy of Sciences, Bratislava, Slovakia*

^d *Cyclotron Institute, Texas A&M University, College Station, Texas, USA*

^e *Laboratori Nazionali del Sud, INFN, Catania, Italy*

* *Corresponding author. Email: soulioti@chem.uoa.gr*

Abstract

This paper presents our recent study on the production of neutron-rich rare isotopes with heavy-ion beams in the energy region of 15 MeV/nucleon. We present calculated production cross sections of neutron-rich nuclides from collisions of a ⁸⁶Kr (15 MeV/nucleon) beam with ²³⁸U targets. Our calculations are based on a two-step approach: the dynamical stage of the collision is described with either the phenomenological Deep-Inelastic Transfer model (DIT), or with the microscopic Constrained Molecular Dynamics model (CoMD). The de-excitation of the hot heavy projectile fragments is performed with the Statistical Multifragmentation Model (SMM). We also performed calculations with a radioactive beam of ⁹²Kr (15 MeV/nucleon) with a target of ²³⁸U and observed that the multinucleon transfer mechanism leads to very neutron-rich nuclides toward and beyond the astrophysical r-process path. In the future, we plan to experimentally investigate such reactions in the KOBRA spectrometer at the RISP facility in Korea. We conclude that the reaction mechanism at beam energies below the Fermi energy involving peripheral nucleon exchange, constitutes a novel and effective route to access extremely neutron-rich isotopes toward the r-process path and the neutron drip-line.

1 Introduction

The exploration of the nuclear landscape toward the astrophysical r-process path and the neutron drip-line have recently received special attention by the nuclear physics community (see, e.g., [1,2] and references therein). Essential to this development is the efficient production of very neutron-rich nuclides which constitutes a central issue in current and upcoming rare isotope beam facilities around the world (see, e.g., [3–12]).

The traditional routes to produce neutron-rich nuclides are spallation, fission and projectile fragmentation [13]. Spallation is an efficient mechanism to produce rare isotopes for ISOL-type techniques [14]. Projectile fission is appropriate in the region of asymmetric fission peaks of the light and heavy fission fragments (see, e.g., [15] for recent efforts on ^{238}U projectile fission). Finally, projectile fragmentation offers a general approach to produce exotic nuclei at beam energies above 100 MeV/nucleon (see, e.g., [16,17]). This approach is, nevertheless, based on the fact that optimum neutron excess in the fragments is achieved by stripping the maximum possible number of protons (and a minimum possible number of neutrons). Surpassing the limits of the traditional approaches and reaching out to the neutron drip line is nowadays highly desirable. Thus, the study of new synthesis routes constitutes a vigorous endeavor of the nuclear community.

Toward this end, to reach a high neutron-excess in the products, apart from proton stripping, it is necessary to capture neutrons from the target. Such a possibility is offered by reactions of nucleon exchange at beam energies from the Coulomb barrier [18,19] to the Fermi energy (20–40 MeV/nucleon) [20,21]. Detailed experimental data in this broad energy range are scarce at present [19,22,23]. In multinucleon transfer and deep-inelastic reactions near the Coulomb barrier [19], the low velocities of the fragments and the wide angular and ionic charge state distributions may limit the collection efficiency for the most neutron-rich products. However, the reactions in the Fermi energy regime combine the advantages of both low-energy (i.e., near and above the Coulomb barrier) and high-energy (i.e., above 100 MeV/nucleon) reactions. At this energy, the interaction of the projectile with the target enhances the N/Z of the fragments, while the velocities are high enough to allow efficient in-flight collection and separation.

Our initial experimental studies of projectile fragments from 25 MeV/nucleon reactions of ^{86}Kr on ^{64}Ni [20] and ^{124}Sn [21] indicated substantial production of neutron-rich fragments. Motivated by recent developments in several facilities that will offer either very intense primary beams [5,8] at this energy range or re-accelerated rare isotope beams [4,5,8,9], we continued our experimental and theoretical studies at 15 MeV/nucleon [24,30–32].

In this contribution, we present calculations of the production cross sections based on either the phenomenological deep-inelastic transfer (DIT) model or the microscopic constrained molecular dynamics model (CoMD). The good description of available experimental results with the DIT code, as well as, with the CoMD code, suggest the possibility of using the present theoretical framework for the prediction of exotic nuclei employing radioactive beams that will soon be available in upcoming facilities. As an example, we present the production cross sections and the rates of neutron-rich nuclei using a radioactive beam of ^{92}Kr at 15 MeV/nucleon interacting with a ^{238}U target.

2 Outline of Results and Comparisons

A detailed presentation of previously obtained experimental results appear in [24] in which the mass spectrometric measurements of production cross sections of neutron-rich projectile fragments from the reactions of a 15 MeV/nucleon ^{86}Kr beam with $^{64,58}\text{Ni}$ and $^{124,112}\text{Sn}$ targets are given. We also note that the experimental results of the 25 MeV/nucleon reactions and the relevant procedures are described in detail in our articles [20–23].

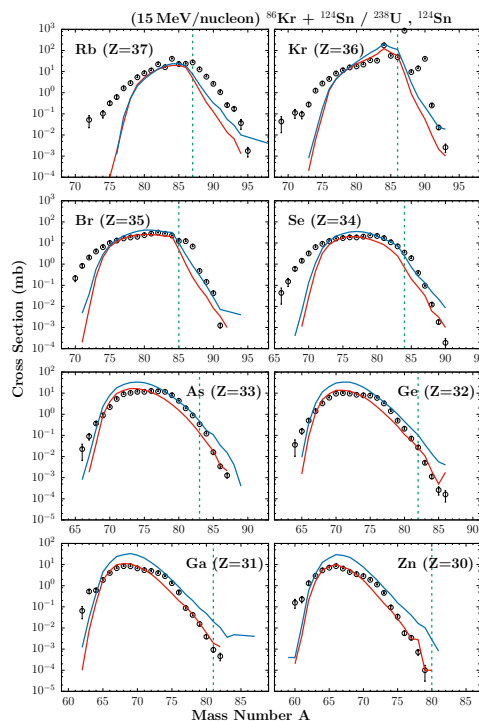


Fig. 1. (Color online) Experimental mass distributions (symbols) of elements with $Z = 37$ – 30 observed in the reaction $^{86}\text{Kr}(15 \text{ MeV/nucleon}) + ^{124}\text{Sn}$ [24] compared to the results of DIT/SMM calculations (solid red line). The solid blue line is the DIT/SMM calculation for the reaction with ^{238}U .

In Fig. 1, we present the experimental mass distributions of elements with

$Z = 37$ – 30 of the reaction $^{86}\text{Kr}(15 \text{ MeV/nucleon}) + ^{124}\text{Sn}$ [24] compared to the calculations with the DIT code [25,26] combined with the de-excitation code SMM [27] (solid red line) used for the de-excitation of the quasiprojectiles emerging after the dynamical stage. The results of the calculations are in overall agreement with the experimental data especially for the isotopes close to the projectile with $Z = 36$ – 32 . Similar agreement is obtained with the microscopic CoMD model [28,29], followed by SMM, but this work is in progress. Furthermore, in Fig. 1 we show the DIT/SMM calculations for the reaction $^{86}\text{Kr}(15 \text{ MeV/nucleon}) + ^{238}\text{U}$. We have chosen the heaviest and most neutron-rich target available in order to explore how far we can go with this reaction. Indeed we observe that the distributions extend further to the right. We note that similar observations were made for the reaction with lighter projectiles on ^{238}U in our recent article [32]. We do not have experimental data for the $^{86}\text{Kr} + ^{238}\text{U}$ reaction, but we have plans to study it in the near future.

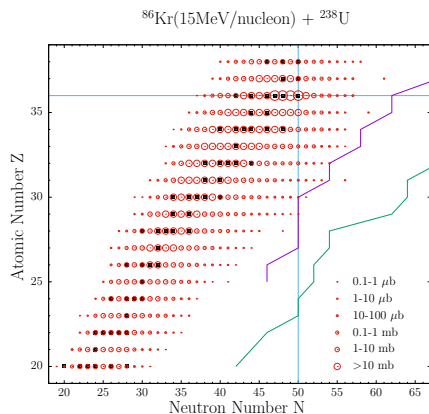


Fig. 2. (Color online) Representation of DIT/SMM calculated production cross sections of projectile fragments from the radioactive-beam reaction ^{86}Kr (15 MeV/nucleon) + ^{238}U on the Z – N plane. The cross section ranges are shown by open circles according to the key. The closed squares show the stable isotopes. The purple line shows the astrophysical r -process path and the green line shows the location of the neutron drip-line. The horizontal and vertical lines indicate, respectively, the proton and neutron number of the ^{86}Kr projectile.

A comprehensive presentation of the DIT/SMM calculated production cross sections of the projectile fragments from the above reaction on the Z vs N plane is given in Fig. 2. In the figure, stable isotopes are represented by closed squares, whereas fragments obtained by the $^{86}\text{Kr} + ^{238}\text{U}$ reaction are given by the open circles (with sizes corresponding to cross-section ranges according to the figure key). The green line gives the location of the neutron drip-line and the purple line indicates the expected path of the astrophysical rapid neutron-capture process (r -process). In the figure, we clearly observe that the neutron pickup products from the ^{86}Kr projectile extend toward the r -process near $Z=30$ – 36 .

After the calculations with the stable ^{86}Kr beam, we proceeded to investigate

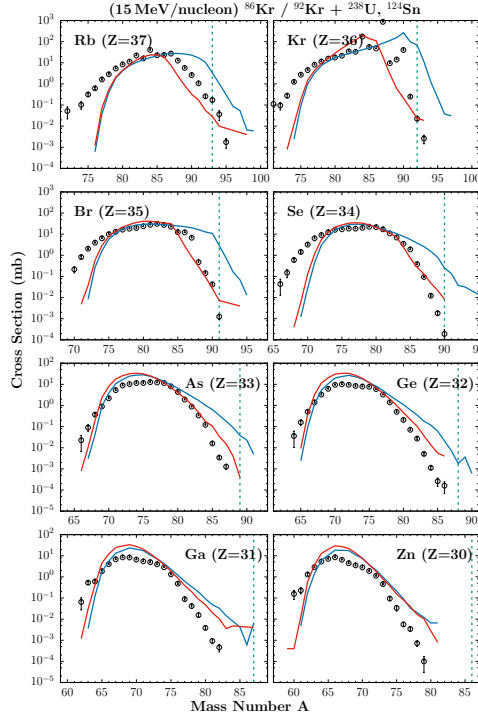


Fig. 3. (Color online) DIT/SMM calculated mass distributions (solid blue line) of elements with $Z = 37-30$ for the reaction $^{92}\text{Kr}(15 \text{ MeV/nucleon}) + ^{238}\text{U}$ compared to the results of DIT/SMM calculations for the reaction with the stable beam ^{86}Kr (solid red line) The experimental mass distributions (symbols) of elements with $Z = 37-30$ from the reaction $^{86}\text{Kr}(15 \text{ MeV/nucleon}) + ^{124}\text{Sn}$ [24] are also given for reference.

what results we would obtain by using a neutron-rich radioactive beam, such as ^{92}Kr . In Fig. 3, we present again the experimental mass distributions (black symbols) of the reaction $^{86}\text{Kr}(15 \text{ MeV/nucleon}) + ^{124}\text{Sn}$, the DIT/SMM calculations for the reaction with $^{86}\text{Kr} + ^{238}\text{U}$ (solid red line) and, furthermore, the DIT/SMM calculations for the reaction $^{92}\text{Kr}(15 \text{ MeV/nucleon}) + ^{238}\text{U}$ (solid blue line). We observe that by using the neutron-rich radioactive beam of ^{92}Kr , we obtain more neutron-rich products. This is primarily true for the isotopes near the projectile. We point out that, e.g., for bromine ($Z=35$), isotopes that have up to 15 more neutrons ($A = 96$) than the corresponding stable isotope ($A = 81$) can be obtained. This observation indicates that by using neutron-rich radioactive beams, and through the mechanism of peripheral multinucleon transfer, we will have the possibility to produce even more neutron-rich nuclides toward the r-process path and the neutron drip line.

A comprehensive presentation of the DIT/SMM calculated production cross sections of the projectile-like fragments from the above radioactive-beam reaction on the Z vs N plane is given in Fig. 4. In this figure, as in Fig. 2, stable isotopes are represented by closed squares, whereas fragments obtained by the radioactive-beam reaction are given by the open circles (with sizes corresponding to cross-section ranges according to the figure key). The green line

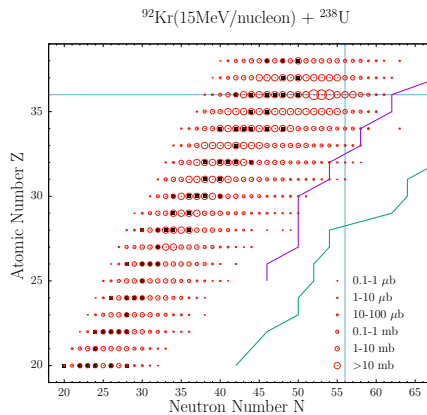


Fig. 4. (Color online) Representation of DIT/SMM calculated production cross sections of projectile fragments from the radioactive-beam reaction ^{92}Kr (15 MeV/nucleon) + ^{238}U on the Z–N plane. The cross section ranges are shown by open circles according to the key. The closed squares show the stable isotopes. The purple line shows the astrophysical r-process path and the green line shows the location of the neutron drip-line. The horizontal and vertical lines indicate, respectively, the proton and neutron number of the ^{92}Kr projectile.

gives the location of the neutron drip-line and the purple line indicates the expected path of the astrophysical rapid neutron-capture process (r-process). In the figure, we observe that the neutron pickup products from ^{92}Kr reach and even exceed the path of the r-process near $Z=30$ – 36 .

In Table I, we present the predicted cross sections and the production rates of neutron rich isotopes from the reaction of the radioactive beam of ^{92}Kr (15 MeV/nucleon) with ^{238}U . For the rate calculations, the ^{92}Kr beam with intensity 1.0 pA (6.2×10^9 particles/sec) is assumed to interact with a ^{238}U target of 20 mg/cm^2 thickness. We see that we have the possibility to produce extremely neutron-rich isotopes in these energies with the use of re-accelerated radioactive beams, such as ^{92}Kr , that will be available in upcoming rare-isotope facilities (e.g. [10–12]). Along these lines, we have plans to continue this work at Texas A&M University (with the MARS separator), at LNS/Catania (using beams from the S800 Cyclotron and the MAGNEX spectrometer) and, in the future, at RISP/Korea (with beams from the RAON accelerator complex and the KOBRA separator).

3 Summary and Conclusions

We presented recent efforts to study the production of neutron-rich rare isotopes with heavy-ion beams in the energy of 15 MeV/nucleon. We first calculated production cross sections of neutron-rich nuclides from collisions of a ^{86}Kr (15 MeV/nucleon) beam with a ^{238}U target. Our calculations are based on a

Table 1

Cross sections and rate estimates (last column) of very neutron-rich isotopes from the reaction ^{92}Kr (15 MeV/nucleon) + ^{238}U . For the rates, a radioactive beam of ^{92}Kr with intensity 1.0 particle nA (6.2×10^9 particles/s) is assumed to interact with a ^{238}U target of 20 mg/cm² thickness.

Rare Isotope	Reaction Channel	Cross Section (mb)	Rate (sec ⁻¹)
^{93}Kr	-0p+1n	12	3.6×10^3
^{94}Kr	-0p+2n	1.3	3.9×10^2
^{95}Kr	-0p+3n	0.3	90
^{96}Kr	-0p+4n	0.05	15
^{92}Br	-1p+1n	0.8	2.4×10^2
^{93}Br	-1p+2n	0.2	60
^{94}Br	-1p+3n	0.07	21
^{95}Br	-1p+4n	0.02	6
^{96}Br	-1p+5n	0.008	2
^{90}Se	-2p+0n	0.25	75
^{91}Se	-2p+1n	0.14	42
^{92}Se	-2p+2n	0.05	15
^{93}Se	-2p+3n	0.02	6

two-step approach: the dynamical stage of the collision is described with either the phenomenological Deep-Inelastic Transfer model (DIT), or with the microscopic Constrained Molecular Dynamics model (CoMD). The de-excitation of the hot heavy projectile fragments is performed with the Statistical Multifragmentation Model (SMM). We also proceeded with calculations with a radioactive beam of ^{92}Kr (15 MeV/nucleon) with ^{238}U and observed that the multinucleon transfer mechanism leads to very neutron-rich nuclides in the mass region of A90–120, toward and beyond the astrophysical r-process path. We conclude that our current understanding of the reaction mechanism at beam energies below the Fermi energy suggests that such nuclear reactions, involving peripheral nucleon exchange, can be exploited as a novel and effective route to access extremely neutron-rich isotopes toward the r-process path and the neutron drip-line. Therefore, future experiments in several accelerator facilities can be planned that will enable a variety of nuclear structure and nuclear reaction studies in unexplored regions of the nuclear chart.

References

- [1] J. Erler et al, Nature **486**, 509 (2011).
- [2] J. Äystö, W. Nazarewicz, M. Pfützner, C. Signorini, eds, Proceedings of the Fifth International Conference on Exotic Nuclei and Atomic Masses (ENAM'08), Ryn, Poland, September 7–13 (2008); Eur. Phys. J. A **42** (2009).
- [3] D. F. Geesaman, C. K. Gelbke, R. V. F. Janssens, B. M. Sherrill, Ann. Rev. Nucl. Part. Sci. **56**, 53 (2006)
- [4] FRIB main page: www.frib.msu.edu
- [5] GANIL main page: www.ganil.fr
- [6] GSI main page: www.gsi.de
- [7] RIBF main page: www.rarf.riken.go.jp/Eng/facilities/RIBF.html
- [8] ATLAS main page: www.phy.anl.gov/atlas/facility/index.html
- [9] EURISOL main page: www.eurisol.org
- [10] RISP main page: www.risp.re.kr/eng/pMainPage.do
- [11] K. Tshoo, Y. K. Kim, Y. K. Kwon et al, Nucl. Instrum. Methods B **317**, 242 (2013).
- [12] K. Tshoo, H. Chae, J. Park, J.Y. Moon, Y.K. Kwon, G.A. Souliotis et al, Nucl. Instrum. Methods B **376**, 188 (2016).
- [13] Y. Blumenfeld, T. Nilsson and P. Van Duppen, Phys. Scr. T152 014023 (2013).
- [14] A. Kelić, M. V. Ricciardi, K. -H. Schmidt, BgNS Transactions, **13**, 98 (2009).
- [15] H. Alvarez-Pol et al., Phys. Rev. C **82**, 041602 (2010).
- [16] O. B. Tarasov et al., Phys. Rev. C **80**, 034609 (2009).
- [17] S. Lukyanov et al., Phys. Rev. C **80**, 014609 (2009).
- [18] V. V. Volkov, Phys. Rep. **44**, 93 (1978).
- [19] L. Corradi, G. Pollarolo, S. Szilner, J. Phys. G **36**, 113101 (2009).
- [20] G. A. Souliotis et al., Phys. Lett. B **543**, 163 (2002).
- [21] G. A. Souliotis et al., Phys. Rev. Lett. **91**, 022701 (2003).
- [22] G. A. Souliotis et al., Nucl. Instrum. Methods **B 204** 166 (2003).
- [23] G. A. Souliotis et al., Nucl. Instrum. Methods **B 266**, 4692 (2008).
- [24] G. A. Souliotis et al., Phys. Rev. C **84**, 064607 (2011).
- [25] L. Tassan-Got and C. Stephan, Nucl. Phys. **A 524**, 121 (1991).

- [26] M. Veselsky and G.A. Souliotis, Nucl. Phys. **A 765**, 252 (2006).
- [27] J. Bondorf et al., Phys. Rep. **257**, 133 (1995).
- [28] M. Papa et al., Phys. Rev. **C 64**, 024612 (2001).
- [29] M. Papa et al, J. Comp. Phys. **208**, 403 (2005).
- [30] P.N. Fountas, G.A. Souliotis, M. Veselsky and A. Bonasera, Phys. Rev. **C 90**, 064613 (2014).
- [31] N. Vonta, G.A. Souliotis et al., Phys. Rev. **C 92**, 064611 (2016).
- [32] A. Papageorgiou, G.A. Souliotis et al., Journal of Physics **G 45**, 095105 (2018).